Muon g-2 and lepton flavor violation in a two Higgs doublets model for the fourth generation

Shaouly Bar-Shalom*

Physics Department, Technion-Institute of Technology, Haifa 32000, Israel

Soumitra Nandi†

Physique des Particules, Université de Montréal, C.P. 6128,
succ. centre-ville, Montréal, QC, Canada H3C 3J7 and
Theoretische Elementarteilchenphysik, Department Physik, Universität Siegen, D-57068 Siegen, Germany

Amarjit Soni‡

Theory Group, Brookhaven National Laboratory, Upton, NY 11973, USA

(Dated: December 19, 2011)

In the minimal Standard Model (SM) with four generations (the so called SM4) and in "standard" two Higgs doublets model (2HDM) setups, e.g., the type II 2HDM with four fermion generations, the contribution of the 4th family heavy leptons to the muon magnetic moment is suppressed and cannot accommodate the measured $\sim 3\sigma$ access with respect to the SM prediction. We show that in a 2HDM for the 4th generation (the 4G2HDM), which we view as a low energy effective theory for dynamical electroweak symmetry breaking, with one of the Higgs doublets coupling only to the 4th family leptons and quarks (thus effectively addressing their large masses), the loop exchanges of the heavy 4th generation neutrino can account for the measured value of the muon anomalous magnetic moment. We also discuss the sensitivity of the lepton flavor violating decays $\mu \to e\gamma$ and $\tau \to \mu\gamma$ and of the decay $B_s \to \mu\mu$ to the new couplings which control the muon g-2 in our model.

PACS numbers:

I. INTRODUCTION

Particle magnetic moments provide an important and valuable test of QED and of the Standard Model (SM). In the case of the muon and the electron magnetic moments, both the experimental measurements and the SM predictions are very precisely known. However, due to its larger mass, the muon magnetic moment is considered more sensitive to massive virtual particles and hence to new physics (NP).

In the SM, the total contributions to the muon $g-2$ (a_μ^{SM}) can be divided into three parts: the QED, the electroweak (EW) and the hadronic contributions. While the QED [1] and EW [2] contributions are well understood, the main theoretical uncertainties lies with the hadronic part which are difficult to control [3]. The hadronic loop contributions cannot be calculated from first principles, so that one relies on a dispersion relation approach [4]. At present the available $\sigma(e^+e^- \to hadrons)$ data are used to calculate the leading-order (LO) and higher-order vacuum polarization contributions to a_μ^{SM}; the estimated contributions are given by [5, 6]

$$a_{LO}^{Had} = 6955(40)(7) \times 10^{-11}, \quad a_{NLO}^{Had,Disp} = -98(1) \times 10^{-11}. \tag{1}$$

On the other hand, the hadronic light-by-light contribution cannot be calculated from data, hence, its evaluation relies on specific models. The latest determination of this term is [7]

$$a_{lbl}^{Had} = 116(39) \times 10^{-11}. \tag{2}$$

Including all these corrections, the complete SM prediction is given by

$$a_\mu^{SM} = 116591834(2)(41)(26) \times 10^{-11} , \tag{3}$$

---

*Electronic address: shaouly@physics.technion.ac.il
†Electronic address: soumitra.nandi@gmail.com
‡Electronic address: soni@bnl.gov

whereas the current experimentally measured value is [8]

$$a_\mu^{exp} = 116592089(54)(33) \times 10^{-11} \,. \tag{4}$$

The SM prediction, therefore, differs from the the experimentally measured value by (see also [9])

$$a_\mu^{\rm new} = a_\mu^{\rm exp} - a_\mu^{\rm SM} = (255 \pm 80) \cdot 10^{-11} \,, \tag{5}$$

which allows some room for new physics. For the purpose of this work we are going to assume that the $\sim 3\sigma$ discrepancy in Eq. 5 is due to NP, although we are aware that the estimates of the hadronic contributions have appreciable uncertainties that may provide part of the discrepancy.

In most extensions of the SM, new charged or neutral states[1], can contribute to the muon anomalous magnetic moment (μAMM) at the one-loop (lowest) level. For example, the μAMM plays an important role in constraining the supersymmetric (SUSY) parameter space, where, as in the SM, the leading SUSY contribution to a_μ arises at one-loop, and is found to be enhanced for large $\tan\beta$. In particular, as was shown in [10], SUSY can address the observed muon $g - 2$ discrepancy for $\tan\beta > 5$ and $\mu > 0$ (Higgsino mass parameter), with typical SUSY masses, of the particles involved in the loops, in the range $100 \text{ GeV} - 500 \text{ GeV}$.

Model independent analysis show that (for details see [9]), for small enough couplings, scalar exchange diagrams could account for the observed μAMM with a scalar mass in the range $480 \text{ GeV} - 690 \text{ GeV}$, whereas pseudoscalar and axial-vector one-loop exchanges contribute with the wrong sign and the one-loop vector exchange contributions are too small.

In this paper we will consider the μAMM in a new 2HDM framework with a heavy 4th generation family. Indeed, we will show that the $\sim 3\sigma$ access (with respect to the SM prediction) shown in Eq. 5 can be explained by one-loop exchanges of the heavy 4th generation neutrino (ν') in a model with two Higgs doublets that we have constructed in [11] and named the 4G2HDM. These new class of two Higgs doublet models were proposed in [11] as viable low energy effective frameworks for models of 4th generation condensation. In particular, a theory with new heavy fermionic states is inevitably cutoff at the near by TeV-scale, where one thus expects some form of strong dynamics and/or compositeness to occur. Thus, as was noted already 20 years ago [12], the low-energy (i.e., sub-TeV) dynamics of such a scenario may be more naturally embedded in multi-Higgs theories, where the new composite scalars are viewed as manifestations of the several possible bound states of the fundamental heavy fermions. Besides, our 4G2HDM can naturally (albeit effectively) accommodate the large (EW-scale) mass of the heavy 4th generation neutrino, which otherwise remains a cause of concern in theories with a 4th family of fermions.

We recall that an additional fourth generation of fermions cannot be ruled out by any symmetry argument, and is not excluded by EW precision data [13]. It is also interesting to note, that already the simplest 4th generation extension of the SM, the so called SM4, has the potential to address some of the current open questions in particle physics, such as the observed baryon asymmetry [14], the Higgs naturalness problem [15], the fermion mass hierarchy problem [16] etc....[2] The SM4 can also accommodate the emerging possible hints for new flavor physics [19–24]. However, the SM4 as such cannot explain the observed muon g-2 discrepancy, see e.g., [25]. In fact, even "standard" 2HDM frameworks (like the type II 2HDM that underlies the minimal SUSY model) with an additional 4th generation of heavy fermions, was shown to fail in explaining the measured μAMM [25].

In section II we calculate the μAMM in the 4G2HDM framework. In sections III and IV we consider the constraints on μAMM from the lepton flavor violating (LFV) decays $\mu \to e\gamma$ and $\tau \to \mu\gamma$ and from $B_s \to \mu\mu$, respectively, and in section V we summarize our results.

II. MUON $g - 2$ IN THE 4G2HDM

At the tree level the muon magnetic moment is predicted by the Dirac equation to be $\vec{M} = g_\mu \frac{e}{2m_\mu} \vec{S}$ with $g_\mu = 2$. The effective vertex of a photon with a charged fermion can in general be written as

$$\bar{u}(p')e\Gamma_\mu u(p) = \bar{u}(p')e \left[\gamma_\mu F_1(q^2) + \frac{i\sigma_{\mu\nu}q^\nu}{2m_f} F_2(q^2) \right] u(p) \,, \tag{6}$$

---

[1] The new states could be a scalar (S), a pseudoscalar (P), a vector (V) or an axial-vector (A).

[2] Note that the neutral Higgs within the SM4 was recently excluded at the LHC in the range $120 \text{ GeV} \lesssim m_H \lesssim 600 \text{ GeV}$ [17]. However, this bound is not relevant to a neutral Higgs of an extended Higgs sector, e.g., a 2HDM framework with four generations of fermions, such as the ones suggested in [11, 18].
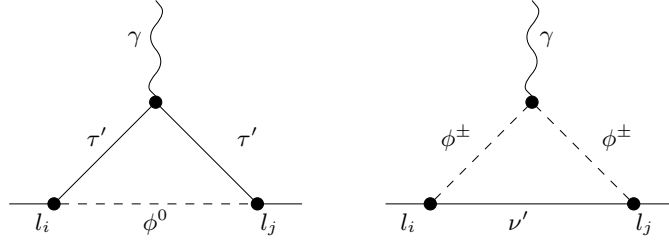
FIG. 1: One-loop diagrams for $l_i \to l_j \gamma$ with charged and neutral scalar exchanges.

where, to lowest order, $F_1(0) = 1$ and $F_2(0) = 0$. While $F_1(0)$ remains unity at all orders due to charge conservation, quantum corrections yield $F_2(0) \neq 0$. Thus, since $g_\mu \equiv 2(F_1(0) + F_2(0))$, it follows that $a_\mu \equiv (g_\mu - 2)/2 = F_2(0)$.

In our 4G2HDM [11] the one-loop contribution to the μAMM can be subdivided as

$$a_\mu = [a_\mu]_W^{SM4} + [a_\mu]_{\mathcal{H}}^{4G2HDM} , \tag{7}$$

where $[a_\mu]_{\mathcal{H}}^{4G2HDM}$ contains the charged and neutral Higgs contributions coming from the one-loop diagrams in Fig. 1 (see below; the diagrams with τ' and ν' in the loop dominate), whereas the SM4-like contribution, $[a_\mu]_W^{SM4}$, comes from the one-loop diagram with $W^\pm - \nu'$ in the loop and is given by [26]

$$\frac{[a_\mu]_W^{SM4}}{|U_{24}|^2} = \frac{G_F m_\mu^2}{4\sqrt{2}\pi^2} A(x_{\nu'}) , \tag{8}$$

where U_{24} is the 24 element of the CKM-like PMNS leptonic matrix, $x_i = m_i^2/M_W^2$ and the loop function $A(x_i)$ is given by

$$A(x_i) = \frac{3x_i^3 \log x_i}{(x_i - 1)^4} + \frac{4x_i^3 - 45x_i^2 + 33x_i - 10}{6(x_i - 1)^3}. \tag{9}$$

For values of $m_{\nu'}$ in the range $100 \text{ GeV} \lesssim m_{\nu'} \lesssim 1000 \text{ GeV}$ one finds $1.5 \times 10^{-9} \lesssim [a_\mu]_W^{SM4}/|U_{24}|^2 \lesssim 3.0 \times 10^{-9}$, so that for $|U_{24}|^2 << 1$ (as expected) the simple SM4 cannot accommodate the observed discrepancy in a_μ.

Let us recapitulate the salient features of the 4G2HDM setups introduced in [11]. In these models one of the Higgs fields (the "heavier" field) couples only to heavy fermionic states, while the second Higgs field (the "lighter" field) is responsible for the mass generation of all other (lighter) fermions. Applying this principle to the 4th generation leptonic sector we have

$$\mathcal{L}_Y = -\bar{E}_L \left(\Phi_\ell Y_e \cdot (I - \mathcal{I}) + \Phi_h Y_e \cdot \mathcal{I} \right) e_R - \bar{E}_L \left(\tilde{\Phi}_\ell Y_\nu \cdot (I - \mathcal{I}) + \Phi_h Y_\nu \cdot \mathcal{I} \right) \nu_R + h.c. , \tag{10}$$

where $f_{L(R)}$ are left(right)-handed fermion fields, E_L is the left-handed $SU(2)$ lepton doublet and Y_e, Y_ν are general 4×4 Yukawa matrices in flavor space. Also, Φ_ℓ and Φ_h are the two Higgs doublets, I is the identity matrix and $\mathcal{I} \equiv \text{diag}(0,0,0,1)$. The Yukawa texture of (10) can be realized in terms of a Z_2-symmetry under which the fields transform as follows: $\Phi_\ell \to -\Phi_\ell$, $\Phi_h \to \Phi_h$, $E_L \to E_L$, $e_R \to -e_R$ (for $e = e, \mu, \tau$), $\nu_R \to -\nu_R$ (for $\nu = \nu_e, \nu_\mu, \nu_\tau$), and $\tau'_R \to \tau'_R$, $\nu'_R \to \nu'_R$.

From the point of view of the leptonic sector, the Yukawa interaction in (10) is the natural underlying setup that can effectively accommodate the heavy masses of the 4th generation leptons, by coupling them to the heavy Higgs doublet. This setup might also be an effective underlying description of more elaborate constructions in models of warped extra dimensions [27].

The Yukawa interactions between the physical Higgs bosons and the leptonic states are then given by (see [11])

$$\mathcal{L}(h\ell_i \ell_j) = \frac{g}{2m_W} \bar{\ell}_i \left\{ m_{\ell_i} \frac{s_\alpha}{c_\beta} \delta_{ij} - f_\beta^h \cdot \left[m_{\ell_i} \Sigma_{ij}^\ell R + m_{\ell_j} \Sigma_{ji}^{\ell*} L \right] \right\} \ell_j h , \tag{11}$$

$$\mathcal{L}(H\ell_i \ell_j) = \frac{g}{2m_W} \bar{\ell}_i \left\{ -m_{\ell_i} \frac{c_\alpha}{c_\beta} \delta_{ij} + f_\beta^H \cdot \left[m_{\ell_i} \Sigma_{ij}^\ell R + m_{\ell_j} \Sigma_{ji}^{\ell*} L \right] \right\} \ell_j H , \tag{12}$$

$$\mathcal{L}(A\ell_i \ell_j) = -iI_{\ell_j} \frac{g}{m_W} \bar{\ell}_i \left\{ m_{\ell_i} \tan\beta \gamma_5 \delta_{ij} - f_\beta \cdot \left[m_{\ell_i} \Sigma_{ij}^\ell R - m_{\ell_j} \Sigma_{ji}^{\ell*} L \right] \right\} \ell_j A , \tag{13}$$

$$\mathcal{L}(H^+ \nu_i e_j) = \frac{g}{\sqrt{2}m_W} \bar{\nu}_i \left\{ \left[m_{e_j} \tan\beta \cdot U_{ji} - m_{e_k} f_\beta \cdot U_{ki} \Sigma_{kj}^e \right] R \right.$$
$$\left. + \left[-m_{\nu_i} \tan\beta \cdot U_{ji} + m_{\nu_k} f_\beta \cdot \Sigma_{ki}^{\nu*} U_{jk} \right] L \right\} e_j H^+ , \tag{14}$$

with

$$f_\beta \equiv \tan\beta + \cot\beta \ , \ \ f_\beta^h \equiv \frac{c_\alpha}{s_\beta} + \frac{s_\alpha}{c_\beta} \ , \ \ f_\beta^H \equiv \frac{c_\alpha}{c_\beta} - \frac{s_\alpha}{s_\beta} \ , \tag{15}$$

and $\tan\beta$ is the ratio between the two VEVs. Also, $H^\pm$ is the charged Higgs, h, H, A are the physical neutral Higgs states (h and H are the lighter and heavier CP-even neutral states, respectively, and A is the neutral CP-odd state), and $\ell = e$ or ν with weak isospin $I_e = -\frac{1}{2}$ and $I_\nu = +\frac{1}{2}$, respectively. Also, $R(L) = \frac{1}{2}(1 + (-)\gamma_5)$ and U is the 4×4 leptonic CKM-like PMNS matrix. Finally, $\Sigma^e(\Sigma^\nu)$ are new mixing matrices in the charged(neutral)-leptonic sectors, obtained after diagonalizing the lepton mass matrices

$$\Sigma^e_{ij} = L^\star_{R,4i} L_{R,4j} \ , \ \ \Sigma^\nu_{ij} = N^\star_{R,4i} N_{R,4j} \ , \tag{16}$$

where L_R, N_R are the rotation (unitary) matrices of the right-handed charged and neutral leptons, respectively. Notice that Σ^e and Σ^ν depend only on the elements of 4th rows of L_R and N_R, respectively, which we will treat as unknowns, i.e., by expressing physical observables in terms of $N_{R,4i}$ and $L_{R,4i}$ or, equivalently in terms of Σ^e_{ij} and Σ^ν_{ij}.[3]

Following [26], let us redefine the Higgs Yukawa interactions as

$$\mathcal{L}(\mathcal{H}\ell_i\ell_j) \equiv \bar{\ell}_i \left[S^\mathcal{H}_{\ell_i\ell_j} + P^\mathcal{H}_{\ell_i\ell_j}\gamma^5 \right] \ell_j \mathcal{H} \ , \tag{17}$$

with $\ell = e$ or ν and $\mathcal{H} = H^+, h, H$ or A. Then, neglecting terms of order $m_e/m_{\tau'}$ for $e = e, \mu, \tau$ and terms of order $\Sigma^\ell_{ij}/\Sigma^\ell_{4k}$ for $i,j,k = 1,2,3$, the above scalar and pseudoscalar couplings, $S^{\mathcal{H}^0}_{\ell_i\tau'}, S^{H^-}_{\ell_i\nu'}$ and $P^{\mathcal{H}^0}_{\ell_i\tau'}, P^{H^-}_{\ell_i\nu'}$ ($i = 1,2$ or 3), which mix the 4th generation leptons with the light leptons, are given in our 4G2HDM by

$$S^{\mathcal{H}^0}_{\ell_i\tau'} = -P^{\mathcal{H}^0}_{\ell_i\tau'} = \frac{g}{4}\frac{m'_\tau}{m_W}F^{\mathcal{H}^0}\Sigma^\nu_{44}\delta_{\Sigma_i} \ ,$$

$$S^{H^-}_{\ell_i\nu'} = \frac{g}{2\sqrt{2}}\frac{m_{\tau'}}{m_W}f_\beta U^*_{44}\Sigma^\nu_{44}\left[\frac{m_{\nu'}}{m_{\tau'}}\left(1 - \frac{t_\beta}{f_\beta\Sigma^\nu_{44}}\right)\delta_{U_i} - \delta_{\Sigma_i}\right] \ ,$$

$$P^{H^-}_{\ell_i\nu'} = -\frac{g}{2\sqrt{2}}\frac{m_{\tau'}}{m_W}f_\beta U^*_{44}\Sigma^\nu_{44}\left[\frac{m_{\nu'}}{m_{\tau'}}\left(1 - \frac{t_\beta}{f_\beta\Sigma^\nu_{44}}\right)\delta_{U_i} + \delta_{\Sigma_i}\right] \ , \tag{18}$$

where $\mathcal{H}^0 = h, H$ or A, $F^h = -f_\beta^h$, $F^H = f_\beta^H$, $F^A = if_\beta$ (see Eq. 15) and

$$\delta_{U_i} \equiv \frac{U^*_{i4}}{U^*_{44}} \ , \ \ \delta_{\Sigma_i} \equiv \frac{\Sigma^{e*}_{4i}}{\Sigma^\nu_{44}} \ , \tag{19}$$

which are the small quantities that parameterize the amount of mixing between the 4th generation leptons and the light leptons of the 1st, 2nd and the 3rd generations. In what follows we will take all quantities in Eq. 18 to be real and always set $U_{44} = \Sigma^\nu_{44} = 1$ and $\tan\beta = 1$ (for limits on $\tan\beta$ in the 4G2HDM see [11]). We note that a_μ and the branching ratios for the LFV decays $\ell_i \to \ell_j\gamma$ are proportional to $1 + \cot^2\beta$ (see Eqs. 22 and 34), so that there is no enhancement for $\tan\beta >> 1$.

Using Eq. 18, the charged and neutral Higgs contributions to a_μ [with $H^\pm - \nu'$ and $\mathcal{H}^0 - \tau'$ in the loop ($\mathcal{H}^0 = h, H$ or A), respectively, see diagrams in Fig. 1] are given by (see also [26])

$$[a_\mu]^{4G2HDM}_{H^\pm} \approx \frac{m_\mu^2}{8\pi^2}\int_0^1 dx \frac{x(x-1)\left\{x\left(\left|S^{H^-}_{\mu\nu'}\right|^2 + \left|P^{H^-}_{\mu\nu'}\right|^2\right) + \frac{m_{\nu'}}{m_\mu}\left(\left|S^{H^-}_{\mu\nu'}\right|^2 - \left|P^{H^-}_{\mu\nu'}\right|^2\right)\right\}}{m_{H^-}^2 x + m_{\nu'}^2(1-x)} \ , \tag{20}$$

$$[a_\mu]^{4G2HDM}_{\mathcal{H}^0} \approx \frac{m_\mu^2}{8\pi^2}\int_0^1 dx \frac{x^2\left\{(1-x)\left(\left|S^{\mathcal{H}^0}_{\mu\tau'}\right|^2 + \left|P^{\mathcal{H}^0}_{\mu\tau'}\right|^2\right) + \frac{m_{\tau'}}{m_\mu}\left(\left|S^{\mathcal{H}^0}_{\mu\tau'}\right|^2 - \left|P^{\mathcal{H}^0}_{\mu\tau'}\right|^2\right)\right\}}{m_{\tau'}^2 x + m_{\mathcal{H}^0}^2(1-x)} \ . \tag{21}$$

[3] Note that since $N_{R,4i}$ and $L_{R,4j}$ parameterize mixings among the 4th generation and the 1st-3rd generations leptons, we expect $\Sigma^\ell_{ij} \ll \Sigma^\ell_{4k}$ for $i,j,k = 1,2,3$, see Eq. 16.

Note that, for the neutral Higgs case, the term proportional to $m_{\nu'}/m_\mu$ vanishes since $|S_{\mu\tau'}^{\mathcal{H}^0}| = |P_{\mu\tau'}^{\mathcal{H}^0}|$ (see Eq. 18). Therefore, the dominant contribution, by far, to a_μ comes from the charged Higgs exchange, in particular, from the second term (proportional to $m_{\nu'}/m_\mu$) in the numerator of Eq. 20, where

$$\left|S_{\mu\nu'}^{H^-}\right|^2 - \left|P_{\mu\nu'}^{H^-}\right|^2 = -\frac{g^2}{2}\frac{m_{\nu'}m_{\tau'}}{m_W^2}f_\beta^2|U_{44}|^2|\Sigma_{44}^\nu|^2 \cdot \mathrm{Re}\left\{\left(1 - \frac{t_\beta}{f_\beta\Sigma_{44}^\nu}\right)\delta_{U_2}\delta_{\Sigma_2}^*\right\} , \tag{22}$$

so that a_μ is proportional to the product $\delta_{\Sigma_2} \cdot \delta_{U_2}$.

In Fig. 2 we plot a_μ as a function of the product $\delta_{\Sigma_2} \cdot \delta_{U_2}$ (assuming its real) for several values of $m_{\nu'}$ and m_{H^+} and fixing $m_{\tau'} = m_{\nu'}$ (a_μ depends linearly on $m_{\tau'}$, see Eq. 22). Depending on the mass $m_{\nu'}$, we find that $\delta_{U_2} \cdot \delta_{\Sigma_2} \sim 10^{-3} - 10^{-2}$ is typically required to accommodate the measured value of a_μ.
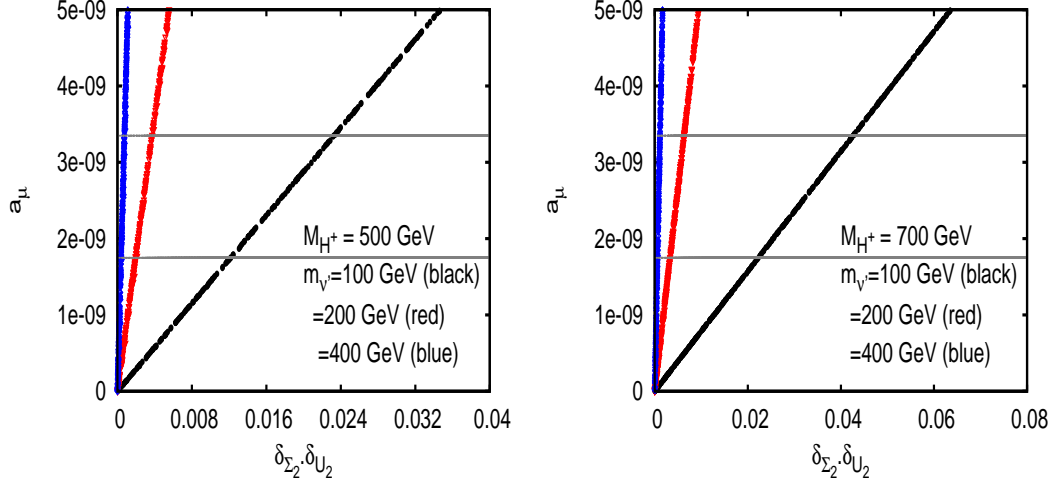

FIG. 2: *The muon $g - 2$ as a function of the product $\delta_{\Sigma_2} \cdot \delta_{U_2}$, for $m_{\nu'} = 100$, 200, 400 GeV, $m_{\tau'} = m_{\nu'}$ and with $m_{H^+} = 500$ GeV (left) and $m_{H^+} = 700$ GeV (right). The horizontal lines are the measured 1-σ bounds on a_μ (see Eq. 4).*

In what follows we will consider the constraints from the lepton flavor violating decays $\ell_i \to \ell_j\gamma$ and from the decay $B_s \to \mu^+\mu^-$, both of which are sensitive to the quantities δ_{U_2} and δ_{Σ_2}, as will be explained below.

III.   CONSTRAINTS FROM LEPTON FLAVOUR VIOLATION

LFV decays such as $\tau \to \mu\gamma$ and $\mu \to e\gamma$, which are absent in the SM, are often found useful for constraining NP models that can potentially contribute to the μAMM, as such processes do not suffer from hadronic uncertainties. The current experimental 90%CL upper bounds on these LFV decays are [8, 28]

$$Br(\tau \to \mu\gamma) < 4.4 \times 10^{-8} \quad , \quad Br(\mu \to e\gamma) < 2.4 \times 10^{-12} . \tag{23}$$

Let us define the amplitude for the transition $\ell_i \to \ell_j\gamma$ as

$$\mathcal{M}(\ell_i \to \ell_j\gamma) = \bar{u}_{\ell_j}(p')\left[i\sigma_{\mu\nu}q^\nu\left(A + B\gamma_5\right)\right]u_{\ell_i}(p)\epsilon^{\mu*} , \tag{24}$$

where $\epsilon^{\mu*}$ is the photon polarization. The decay width is then given by

$$\Gamma(\ell_i \to \ell_j\gamma) = \frac{m_{\ell_i}^3}{8\pi}\left(1 - \frac{m_{\ell_j}^2}{m_{\ell_i}^2}\right)\left[\left(1 + \frac{m_{\ell_j}^2}{m_{\ell_i}^2}\right)\left(|A|^2 + |B|^2\right) + 4\frac{m_{\ell_j}}{m_{\ell_i}}\left(|A|^2 - |B|^2\right)\right] . \tag{25}$$

Here again, the new 4G2HDM amplitude $\mathcal{M}(\ell_i \to \ell_j\gamma)^{4G2HDM}$ can be divided as

$$\mathcal{M}(\ell_i \to \ell_j\gamma)^{4G2HDM} \equiv \mathcal{M}_W^{SM4}(\ell_i \to \ell_j\gamma) + \mathcal{M}_{H^+}^{4G2HDM}(\ell_i \to \ell_j\gamma) + \mathcal{M}_{\mathcal{H}^0}^{4G2HDM}(\ell_i \to \ell_j\gamma) , \tag{26}$$

where $\mathcal{M}_W^{SM4}(\ell_i \to \ell_j\gamma)$ are the SM4-like W-exchange contribution which is obtained from the diagram (right) of Fig. 1 with $\phi^\pm$ replaced by $W^\pm$ plus the diagrams which contain the self-energy corrections to the external fermion line ℓ_i or ℓ_j. In particular, using the definition in Eq. 24 and taking the limit $m_{\ell_j} \to 0$, the net contribution to $\mathcal{M}_W^{SM4}(\ell_i \to \ell_j\gamma)$ with internal ν' in the loop is given by [29]

$$A_W^{SM4} = B_W^{SM4} = \frac{eG_F m_{\ell_i}}{4\sqrt{2}\pi^2} U_{j4} U_{i4}^* F(x_{\nu'}) , \qquad (27)$$

where $x_i = m_i^2/M_W^2$ and $F(x_i)$ is given by

$$F(x_i) = \frac{x_i(1 - 6x_i + 3x_i^2 + 2x_i^3 - 6x_i^2 \log x_i)}{4(1-x_i)^4} . \qquad (28)$$

Here also, we find that $\mathcal{M}_W^{SM4}(\ell_i \to \ell_j\gamma)$ is much smaller than the charged and neutral Higgs amplitudes, $\mathcal{M}_{H^+}^{4G2HDM}(\ell_i \to \ell_j\gamma)$ and $\mathcal{M}_{\mathcal{H}^0}^{4G2HDM}(\ell_i \to \ell_j\gamma)$ (calculated from the diagrams in Fig. 1), for which we obtain

$$A_{H^-}^{4G2HDM} = \frac{e}{32\pi^2}\left\{(m_{\ell_i}+m_{\ell_j})\left(S_{\ell_i\nu'}^{H^-}{}^* S_{\ell_j\nu'}^{H^-} + P_{\ell_i\nu'}^{H^-}{}^* P_{\ell_j\nu'}^{H^-}\right) I_1^{H^+} + 2m_{\nu'}\left(S_{\ell_i\nu'}^{H^-}{}^* S_{\ell_j\nu'}^{H^-} - P_{\ell_i\nu'}^{H^-}{}^* P_{\ell_j\nu'}^{H^-}\right) I_2^{H^+}\right\} ,(29)$$

$$B_{H^-}^{4G2HDM} = \frac{e}{32\pi^2}\left\{(m_{\ell_i}-m_{\ell_j})\left(S_{\ell_i\nu'}^{H^-}{}^* P_{\ell_j\nu'}^{H^-} + S_{\ell_j\nu'}^{H^-} P_{\ell_i\nu'}^{H^-}{}^*\right) I_1^{H^+} + 2m_{\nu'}\left(S_{\ell_i\nu'}^{H^-}{}^* P_{\ell_j\nu'}^{H^-} - S_{\ell_j\nu'}^{H^-} P_{\ell_i\nu'}^{H^-}{}^*\right) I_2^{H^+}\right\} ,(30)$$

$$A_{\mathcal{H}^0}^{4G2HDM} = \frac{e}{32\pi^2}\left\{(m_{\ell_i}+m_{\ell_j})\left(S_{\ell_i\tau'}^{\mathcal{H}^0}{}^* S_{\ell_j\tau'}^{\mathcal{H}^0} + P_{\ell_i\tau'}^{\mathcal{H}^0}{}^* P_{\ell_j\tau'}^{\mathcal{H}^0}\right) I_1^{\mathcal{H}^0} + 2m_{\tau'}\left(S_{\ell_i\tau'}^{\mathcal{H}^0}{}^* S_{\ell_j\tau'}^{\mathcal{H}^0} - P_{\ell_i\tau'}^{\mathcal{H}^0}{}^* P_{\ell_j\tau'}^{\mathcal{H}^0}\right) I_2^{\mathcal{H}^0}\right\} , (31)$$

$$B_{\mathcal{H}^0}^{4G2HDM} = \frac{e}{32\pi^2}\left\{(m_{\ell_i}-m_{\ell_j})\left(S_{\ell_i\tau'}^{\mathcal{H}^0}{}^* P_{\ell_j\tau'}^{\mathcal{H}^0} + S_{\ell_j\tau'}^{\mathcal{H}^0} P_{\ell_i\tau'}^{\mathcal{H}^0}{}^*\right) I_1^{\mathcal{H}^0} + 2m_{\tau'}\left(S_{\ell_i\tau'}^{\mathcal{H}^0}{}^* P_{\ell_j\tau'}^{\mathcal{H}^0} - S_{\ell_j\tau'}^{\mathcal{H}^0} P_{\ell_i\tau'}^{\mathcal{H}^0}{}^*\right) I_2^{\mathcal{H}^0}\right\} , (32)$$

where the loop integrals $I_1^{H^+}$, $I_2^{H^+}$, $I_1^{\mathcal{H}^0}$ and $I_2^{\mathcal{H}^0}$ are given by (taking $m_{\ell_i}^2, m_{\ell_j}^2 \ll m_{\mathcal{H}}^2, m_{\nu'}^2, m_{\tau'}^2$):

$$\begin{aligned}
I_1^{H^+} &\approx \int_0^1 dx \frac{x^2(x-1)}{m_{H^-}^2 x + m_{\nu'}^2(1-x)} , \\
I_2^{H^+} &\approx \int_0^1 dx \frac{x(x-1)}{m_{H^-}^2 x + m_{\nu'}^2(1-x)} , \\
I_1^{\mathcal{H}^0} &\approx \int_0^1 dx \frac{x^2(1-x)}{m_{\tau'}^2 x + m_{\mathcal{H}^0}^2(1-x)} , \\
I_2^{\mathcal{H}^0} &\approx \int_0^1 dx \frac{x^2}{m_{\tau'}^2 x + m_{\mathcal{H}^0}^2(1-x)} .
\end{aligned} \qquad (33)$$

The dominant terms in Eqs. 29-32 are the ones proportional to $m_{\nu'}$ from the charged Higgs exchange contribution,

$$\begin{aligned}
\left(S_{\ell_i\nu'}^{H^-}{}^* S_{\ell_j\nu'}^{H^-} - P_{\ell_i\nu'}^{H^-}{}^* P_{\ell_j\nu'}^{H^-}\right) &= -\frac{g^2}{4}\frac{m_{\nu'}m_{\tau'}}{m_W^2} f_\beta^2 |U_{44}|^2 |\Sigma_{44}^\nu|^2 \left(1 - \frac{t_\beta}{f_\beta \Sigma_{44}^\nu}\right)\left(\delta_{U_i}^* \delta_{\Sigma_j} + \delta_{U_j}\delta_{\Sigma_i}^*\right) , \\
\left(S_{\ell_i\nu'}^{H^-}{}^* P_{\ell_j\nu'}^{H^-} - S_{\ell_i\nu'}^{H^-}{}^* P_{\ell_j\nu'}^{H^-}\right) &= -\frac{g^2}{4}\frac{m_{\nu'}m_{\tau'}}{m_W^2} f_\beta^2 |U_{44}|^2 |\Sigma_{44}^\nu|^2 \left(1 - \frac{t_\beta}{f_\beta \Sigma_{44}^\nu}\right)\left(\delta_{U_i}^* \delta_{\Sigma_j} - \delta_{U_j}\delta_{\Sigma_i}^*\right) , \qquad (34)
\end{aligned}$$

since the terms proportional to $m_{\tau'}$ in the neutral Higgs exchanges vanish due to $|S_{\ell_i\tau'}^{\mathcal{H}^0}| = |P_{\ell_i\tau'}^{\mathcal{H}^0}|$ (see Eq. 18).

We thus find that in our 4G2HDM, the decays $\mu \to e\gamma$ and $\tau \to \mu\gamma$ are sensitive to δ_{U_2} and δ_{Σ_2} through the products $(\delta_{U_2}\delta_{\Sigma_1}, \delta_{U_1}\delta_{\Sigma_2})$ and $(\delta_{U_3}\delta_{\Sigma_2}, \delta_{U_2}\delta_{\Sigma_3})$, respectively, so that, in principle, one can avoid constraints on the quantities δ_{U_2} and δ_{Σ_2} if $\delta_{U_1}, \delta_{U_3}, \delta_{\Sigma_1}$ and δ_{Σ_3} are sufficiently small.

In Figs. 3 we plot $BR(\mu \to e\gamma)$ as a function of $\delta_{U_1} \cdot \delta_{\Sigma_2}$ and $\delta_{U_2} \cdot \delta_{\Sigma_1}$, for $m_{\nu'} = 100$, 200, 400 GeV, $m_{H^+} = 500$ GeV and fixing $m_{\tau'} = m_{\nu'}$. We see that for e.g. $m_{\nu'} = 100$ GeV and for values of δ_{U_2} and δ_{Σ_2} of $\mathcal{O}(0.1)$ [for which the product $\delta_{U_2} \cdot \delta_{\Sigma_2}$ reproduces the measured a_μ (see Fig. 2)], δ_{U_1} and δ_{Σ_1} are required to be smaller than few $\times 10^{-5}$, implying that $\delta_{U_1} \ll \delta_{U_2}$ and $\delta_{\Sigma_1} \ll \delta_{\Sigma_2}$.

In Fig. 4 we plot $BR(\tau \to \mu\gamma)$ as a function of $\delta_{U_2} \cdot \delta_{\Sigma_3}$ and $\delta_{U_3} \cdot \delta_{\Sigma_2}$, and in Fig. 5 we give a scatter plot of the allowed values in the $\delta_{\Sigma_3} - \delta_{U_3}$ plane, for which $BR(\tau \to \mu\gamma) < 4.4 \times 10^{-8}$ (i.e., below its 90%CL bound). In both plots we use $m_{\nu'} = 100$, 200, 400 GeV, $m_{H^+} = 500$ GeV and we fix $m_{\tau'} = m_{\nu'}$. The individual couplings δ_{U_2} and δ_{Σ_2} are randomly chosen to always be within values that reproduce the measured a_μ (see Fig. 2). We see that the products $\delta_{U_2} \cdot \delta_{\Sigma_3}$ and $\delta_{U_3} \cdot \delta_{\Sigma_2}$ are required to be at most few $\times 0.001$, in order to be consistent with the current bounds on $BR(\tau \to \mu\gamma)$.
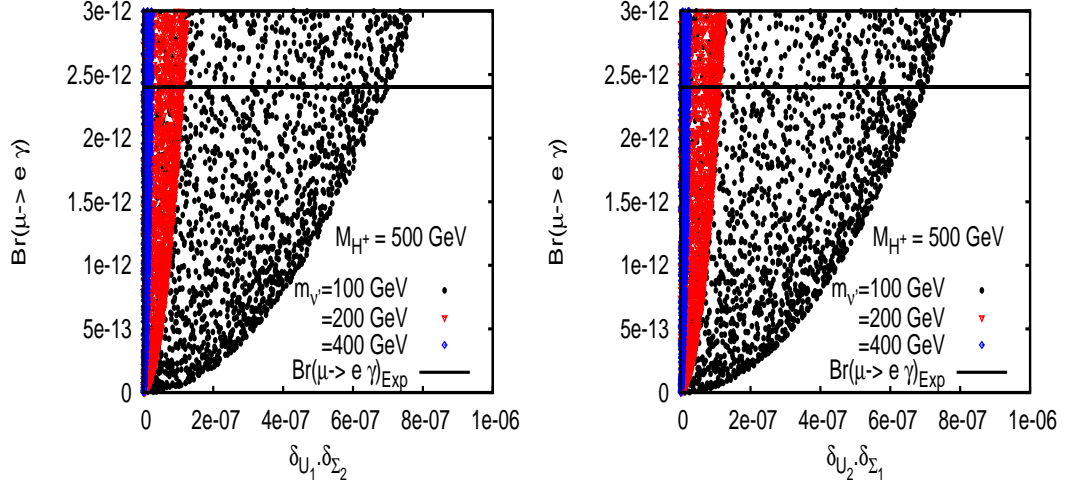
FIG. 3: $BR(\mu \to e\gamma)$ as a function of $\delta_{U_1} \cdot \delta_{\Sigma_2}$ (left) and of $\delta_{U_2} \cdot \delta_{\Sigma_1}$ (right), for $m_{\nu'} = 100$, 200, 400 GeV, $m_{\tau'} = m_{\nu'}$ and with $m_{H^+} = 500$ GeV. Also shown (horizontal line) is the 90%CL upper limit on $BR(\mu \to e\gamma)$ (see Eq. 23).
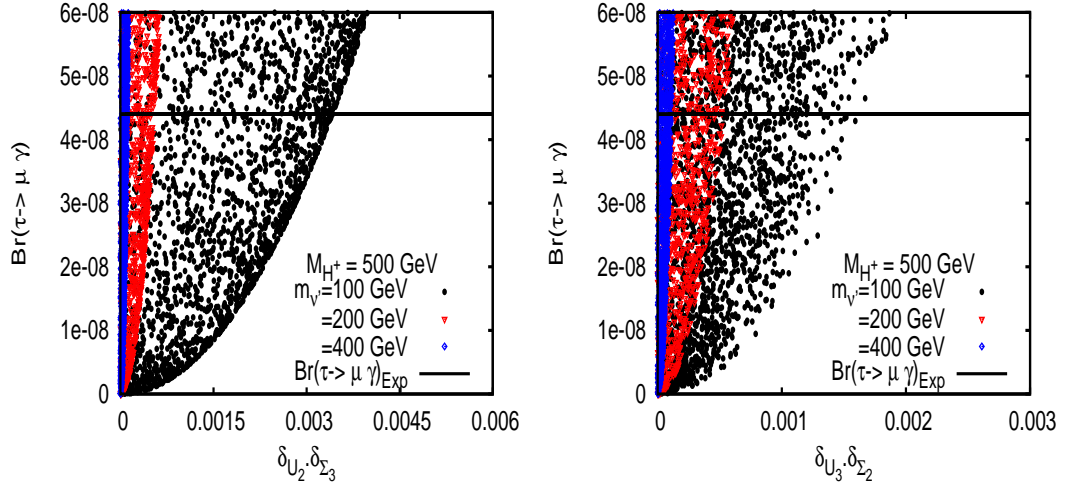

FIG. 4: $BR(\tau \to \mu\gamma)$ as a function of $\delta_{U_3} \cdot \delta_{\Sigma_2}$ (left) and $\delta_{U_2} \cdot \delta_{\Sigma_3}$ (right), for $m_{\nu'} = 100$, 200, 400 GeV, $m_{\tau'} = m_{\nu'}$ and with $m_{H^+} = 500$ GeV. Also shown (horizontal line) is the 90%CL upper limit on $BR(\tau \to \mu\gamma)$ (see Eq. 23).

We can thus identify a typical benchmark texture for the 4th generation elements of the CKM-like PMNS matrix, U_{i4}, and for the new mixing matrix Σ_{4i}^e that can explain the observed μAMM and still be consistent with the current LFV constraints

$$U_{i4} \sim \left(\Sigma_{4i}^e\right)^T \simeq \begin{pmatrix} \epsilon^5 \\ \epsilon \\ \epsilon^2 \\ 1 \end{pmatrix} \,, \tag{35}$$

where e.g., $\epsilon \sim 0.1$ for $m_{\nu'} = 100$ GeV.

Admittedly, the above texture implies a hierarchical pattern which is different from the observed hierarchy in the quark's CKM matrix - usually termed as "normal". Nonetheless, without a fundamental theory of flavor, our insights for flavor should be data driven also in the leptonic sector. Besides, the above texture is sensitive to the current precision in the measurement of the muon g-2 which can change e.g., if more accurate calculations end up showing that part of the hadronic contributions cannot be ignored.
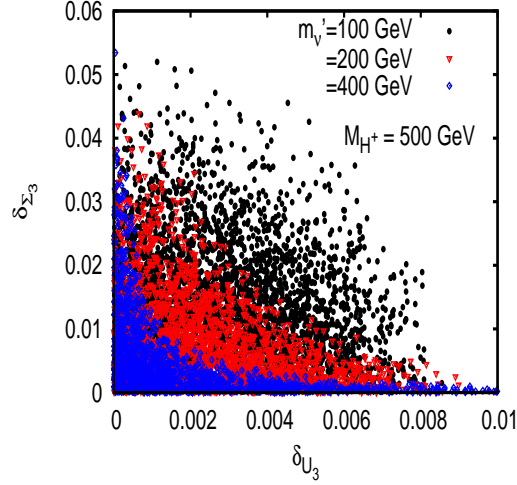
FIG. 5: *Allowed values in the $\delta_{\Sigma_3} - \delta_{U_3}$ plane, for which $BR(\tau \to \mu\gamma) < 4.4 \times 10^{-8}$ (i.e., below its 90%CL bound), for $m_{\nu'} = 100, 200, 400$ GeV, $m_{\tau'} = m_{\nu'}$ and with $m_{H^+} = 500$ GeV. The couplings δ_{U_2} and δ_{Σ_2} are chosen randomly in the range $[0, 0.2]$ so that the product $\delta_{U_2} \cdot \delta_{\Sigma_2}$ reproduces the measured a_μ (see Fig. 2).*

$m_{\nu'}$ (GeV)	$\delta_{U_2} = \delta_{\Sigma_2}$	a_μ $\times 10^9$	$\mathrm{Br}(\mu \to e\gamma)$ $\times 10^{12}$	$\delta_{U_1}.\delta_{\Sigma_2}$ $\times 10^7$	$\delta_{U_2}.\delta_{\Sigma_1}$ $\times 10^7$	$\mathrm{Br}(\tau \to \mu\gamma)$ $\times 10^8$	$\delta_{U_3}.\delta_{\Sigma_2}$ $\times 10^4$	$\delta_{U_2}.\delta_{\Sigma_3}$ $\times 10^4$
100	0.12	2.07	1.20	1.31	4.57	1.78	1.85	20.40
			0.64	2.45	2.25	0.77	3.21	5.90
			0.14	1.51	0.45	0.26	2.00	2.12
200	0.05	2.25	1.21	0.22	0.76	2.03	0.51	3.65
			0.62	0.51	0.25	0.79	0.41	2.25
			0.11	0.43	0.61	0.18	0.16	1.07
400	0.022	2.19	1.39	0.16	0.04	2.14	0.73	0.12
			0.69	0.07	0.10	0.78	0.40	0.21
			0.17	0.05	0.02	0.13	0.11	0.14

TABLE I: The calculated a_μ and the branching fractions for the LFV decays $\tau \to \mu\gamma$ and $\mu \to e\gamma$ in the 4G2HDM, for several representative values of the couplings δ_{U_2}, δ_{Σ_2} and the products $(\delta_{U_1}.\delta_{\Sigma_2})$, $(\delta_{U_2}.\delta_{\Sigma_1})$, $(\delta_{U_3}.\delta_{\Sigma_2})$ and $(\delta_{U_2}.\delta_{\Sigma_3})$ that are consistent with the measured μAMM and which give $\mathrm{Br}(\tau \to \mu\gamma)$ and $\mathrm{Br}(\mu \to e\gamma)$ at the level of $\mathcal{O}(10^{-13})$ and $\mathcal{O}(10^{-9})$, respectively.

In Table I we list several representative values of the couplings δ_{U_2}, δ_{Σ_2} and the products $(\delta_{U_1}, \delta_{\Sigma_2})$, $(\delta_{U_2}, \delta_{\Sigma_1})$, $(\delta_{U_3}, \delta_{\Sigma_2})$ and $(\delta_{U_2}, \delta_{\Sigma_3})$ that are consistent with the measured μAMM (i.e., a_μ^{exp} given in eq. 4), and that give LFV branching fractions $\mathrm{Br}(\tau \to \mu\gamma)$ and $\mathrm{Br}(\mu \to e\gamma)$ at the level of $\mathcal{O}(10^{-13})$ and $\mathcal{O}(10^{-9})$, respectively, that are accessible to near future experiments [28, 30].

IV. CONSTRAINTS FROM $B_s \to \ell^+\ell^-$

In the SM, tree level $b \to s$ FCNC transitions are forbidden, and also the purely leptonic $B_s \to \ell^+\ell^-$ decays, with $\ell = e, \mu, \tau$, suffer from chiral suppression and are therefore very sensitive to new physics. The SM predicted branching fractions for these decays are appreciably smaller than those of the semi-leptonic decays. For example, for $B_s \to \mu^+\mu^-$, the SM prediction is [21]

$$Br(B_s \to \mu^+\mu^-) = (3.2 \pm 0.2) \cdot 10^{-9} \ . \tag{36}$$

In the LHC era the current limit on $Br(B_s \to \mu^+\mu^-)$ has been improved. A combined analysis by LHCb and CMS, using $0.34 fb^{-1}$ and $1.14 fb^{-1}$ data sample, respectively, yields [31]

$$Br(B_s \to \mu^+\mu^-) < 1.08 \times 10^{-8} \ , \qquad (LHCb + CMS)@95\%CL \tag{37}$$
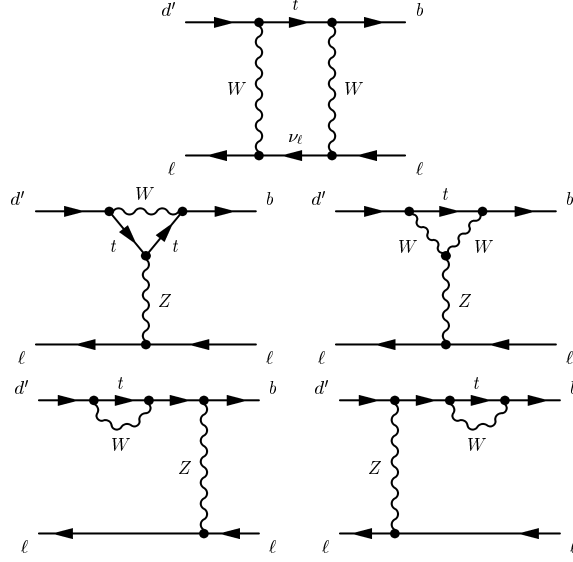
FIG. 6: Dominant SM diagrams in the $B_{d'} \to \ell^+\ell^-$ decay.

whereas the same measurement by CDF-II, using a $7fb^{-1}$ data sample, gives [32]

$$Br(B_s \to \mu^+\mu^-) < 4.0 \times 10^{-8} \qquad CDF@95\%CL. \tag{38}$$

In fact, LHCb has the sensitivity to measure the $Br(B_s \to \mu^+\mu^-)$ down to $\sim 2 \times 10^{-9}$, which is about 5σ smaller than the SM prediction.

In general, the matrix element for the decay $\bar{B}_s \to \ell^+\ell^-$ can be written as [33]

$$\mathcal{M} = \frac{G_F\alpha}{2\sqrt{2}\pi \sin\theta_W^2} \left[F_S\, \bar{\ell}\ell + F_P\, \bar{\ell}\gamma_5\ell + F_A\, P^\mu\bar{\ell}\gamma_\mu\gamma_5\ell \right], \tag{39}$$

where P^μ is the four momentum of the initial B_s meson and F_i's are functions of Lorentz invariant quantities. Squaring the matrix and summing over the lepton spins, we obtain the branching fraction

$$Br(\bar{B}_s \to \ell^+\ell^-) = \frac{G_F^2\alpha^2 M_{B_s}\tau_{B_s}}{64\pi^3}\sqrt{1 - \frac{4m_\ell^2}{M_{B_s}^2}}\left[\left(1 - \frac{4m_\ell^2}{M_{B_s}^2}\right)|F_S|^2 + |F_P + 2m_\ell F_A|^2\right]. \tag{40}$$

In the SM, the dominant effect in $\bar{B}_s \to \ell^+\ell^-$ arise from the diagrams shown in Fig. 6, which contribute to F_A in Eq. 39. At next-to-leading (NLO) QCD corrections, the net contribution in F_A is given by [34, 35]

$$F_A^{SM} = -i\, f_{B_s}\, V_{tb}V_{ts}^*\, Y(x_t) = -i\, f_{B_s}\, V_{tb}V_{ts}^* \times 0.997\left[\frac{m_t(m_t)}{166\text{GeV}}\right]^{1.55}. \tag{41}$$

In the SM4 it is again F_A which receives a non-zero contribution:

$$F_A^{SM4} = (F_A^{SM4})^{peng} + (F_A^{SM4})^{box}, \tag{42}$$

where $(F_A^{SM4})^{peng}$ is the contributions from the Z-penguin diagrams in Fig. 6 with the top quark replaced by a t', and $(F_A^{SM4})^{box}$ is the contribution from the box diagram in Fig. 6 with the replacement $t \to t'$ and $\nu_\ell \to \nu'$. At leading-order (LO) in QCD, they are given by

$$(F_A^{SM4})^{peng} = -i\, f_{B_s}V_{t'b}V_{t's}^*\frac{x_{t'}}{8}\left[\frac{6 - x_{t'}}{1 - x_{t'}} + \frac{3x_{t'} + 2}{(1 - x_{t'})^2}\ln x_{t'}\right], \tag{43}$$

$$(F_A^{SM4})^{box} = -i\, f_{B_s}\, V_{t'b}V_{t's}^*\, |U_{24}|^2\frac{B_0(x_{t'}, x_{\nu'})}{4}, \tag{44}$$

with

$$B_0(x_i, x_j) = x_i\, x_j \left[-\frac{3}{4}\frac{1}{(1-x_i)(1-x_j)} + \frac{\ln x_i}{(x_i - x_j)(1-x_i)^2}\left(1 - 2x_i + \frac{x_i^2}{4}\right) \right.$$
$$\left. + \frac{\ln x_j}{(x_j - x_i)(1-x_j)^2}\left(1 - 2x_j + \frac{x_j^2}{4}\right) \right]. \tag{45}$$

In our 4G2HDM, we have additional contributions to F_A coming from the charged Higgs exchange penguin and box diagrams (replacing $W^+ \to H^+$ in Fig. 6) and, in addition, there are new contributions to F_S and F_P. For our purpose, we are interested only in the diagrams that are sensitive to the $\ell^\pm \nu' H^\pm$ vertex, which are, therefore, directly related to the muon g-2. The dominant diagrams that contribute to the $\bar{B}_s \to \ell^+\ell^-$ decay with this vertex are the Higgs-exchange box diagrams in Fig. 6, where one or two W-bosons are replaced by H^+ and (t, ν_ℓ) are being replaced by both (t, ν') and (t', ν'). Thus, the net contributions to F_S, F_P and F_A in Eq. 39 can be written as

$$F_S = F_S^H, \quad F_P = F_P^H \quad and \quad F_A = F_A^{SM} + F_A^{SM4} + F_A^H\,, \tag{46}$$

where F_S^H, F_P^H and F_A^H are the contributions from the dominant new Higgs-exchange box diagrams, which, for the (t', ν') exchange, are given by

$$F_S^H = (F_S)_{HH}^{box} + (F_S)_{WH}^{box},$$
$$= -\frac{i\,2f_{B_s}}{g^2}\frac{M_{B_s}^2}{m_b + m_s}\left[\frac{m_{\nu'}m_{t'}}{M_{H^-}^4}\left(S_{t's}^{H^{-}*}P_{t'b}^{H^-} - S_{t'b}^{H^-}P_{t's}^{H^{-}*}\right)\left(\left|S_{\mu\nu'}^{H^-}\right|^2 - \left|P_{\mu\nu'}^{H^-}\right|^2\right)B_{HH}^S(y_{t'}, y_{\nu'}) \right.$$
$$+ \frac{g}{2\sqrt{2}m_W}\left\{V_{t'b}U_{24}^*\left(S_{t's}^{H^{-}*} + P_{t's}^{\mathcal{H}*}\right)\left(S_{\mu\nu'}^{H^-} + P_{\mu\nu'}^{H^-}\right) - V_{t's}^*U_{24}\left(S_{t'b}^{H^-} + P_{t'b}^{H^-}\right)\right.$$
$$\left.\left.\left(S_{\mu\nu'}^{H^{-}*} + P_{\mu\nu'}^{H^{-}*}\right)\right\}B_{WH}^S(x_{t'}, x_{\nu'}, x_H) \right] \tag{47}$$

$$F_P^H = (F_P)_{HH}^{box} + (F_P)_{WH}^{box},$$
$$= -\frac{i\,2f_{B_s}}{g^2}\frac{M_{B_s}^2}{m_b + m_s}\left[\frac{m_{\nu'}m_{t'}}{M_{H^-}^4}\left(S_{t's}^{H^{-}*}P_{t'b}^{H^-} - S_{t'b}^{H^-}P_{t's}^{H^{-}*}\right)\left(P_{\mu\nu'}^{H^-}S_{\mu\nu'}^{H^{-}*} - S_{\mu\nu'}^{H^-}P_{\mu\nu'}^{H^{-}*}\right)B_{HH}^P(y_{t'}, y_{\nu'}) \right.$$
$$+ \frac{g}{2\sqrt{2}m_W}\left\{V_{t'b}U_{24}^*\left(S_{t's}^{H^{-}*} + P_{t's}^{H^{-}*}\right)\left(S_{\mu\nu'}^{H^-} + P_{\mu\nu'}^{H^-}\right) + V_{t's}^*U_{24}\left(S_{t'b}^{H^-} + P_{t'b}^{H^-}\right)\right.$$
$$\left.\left.\left(S_{\mu\nu'}^{H^{-}*} + P_{\mu\nu'}^{H^{-}*}\right)\right\}B_{WH}^P(x_{t'}, x_{\nu'}, x_H) \right] \tag{48}$$

$$F_A^H = (F_A)_{HH}^{box} + (F_A)_{WH}^{box},$$
$$= -\frac{i\,2f_{B_s}}{g^2}\left[\frac{1}{4\,M_{H^-}^2}\left(S_{t's}^{H^-}P_{t'b}^{H^{-}*} + S_{t'b}^{H^{-}*}P_{t's}^{H^-}\right)\left(P_{\mu\nu'}^{H^-}S_{\mu\nu'}^{H^{-}*} + S_{\mu\nu'}^{H^-}P_{\mu\nu'}^{H^{-}*}\right)B_{HH}^A(y_{t'}, y_{\nu'}) \right.$$
$$+ \frac{g}{2\sqrt{2}m_W}\frac{m_{\nu'}m_{t'}}{m_W^2}\left\{V_{t'b}U_{24}^*\left(P_{t's}^{H^{-}*} - S_{t's}^{H^{-}*}\right)\left(S_{\mu\nu'}^{H^-} - P_{\mu\nu'}^{H^-}\right) + V_{t's}^*U_{24}\left(P_{t'b}^{H^-} - S_{t'b}^{H^-}\right)\right.$$
$$\left.\left.\left(S_{\mu\nu'}^{H^{-}*} - P_{\mu\nu'}^{H^{-}*}\right)\right\}B_{WH}^A(x_{t'}, x_{\nu'}, x_H) \right], \tag{49}$$

where $y_i = m_i^2/M_{H^-}^2$, $x_i = m_i^2/M_W^2$ and the loop-functions are given by

$$B_{HH}^S(y_i, y_j) = B_{HH}^P(y_i, y_j) = \frac{1}{y_i - y_j}\left\{\frac{y_j \ln y_j}{(1-y_j)^2} - \frac{y_i \ln y_i}{(1-y_i)^2}\right\} - \frac{1}{(1-y_i)(1-y_j)}$$

$$B_{WH}^S(x_i, x_j, x_H) = B_{WH}^P(x_i, x_j, x_H) = \frac{x_H^2 \ln x_H}{(x_H - 1)(x_H - x_i)(x_H - x_j)}$$
$$+ \frac{x_i^2 \ln x_i}{(x_i - 1)(x_i - x_H)(x_i - x_j)} + \frac{x_j^2 \ln x_j}{(x_j - 1)(x_j - x_H)(x_j - x_i)}$$

$$B_{HH}^A(y_i, y_j) = \frac{y_j^2 \ln y_j}{(1-y_j)^2\,(y_j - y_i)} + \frac{y_i^2 \ln y_i}{(1-y_i)^2\,(y_i - y_j)} + \frac{1}{(1-y_i)(1-y_j)}$$

$$B_{WH}^A(x_i, x_j, x_H) = \frac{x_H \ln x_H}{(x_H - 1)(x_H - x_i)(x_H - x_j)} + \frac{x_i \ln x_i}{(x_i - 1)(x_i - x_H)(x_i - x_j)}$$
$$+ \frac{x_j \ln x_j}{(x_j - 1)(x_j - x_H)(x_j - x_i)}\,. \tag{50}$$

Also, $S_{\mu\nu'}^{H^-}$, $P_{\mu\nu'}^{H^-}$ are defined in Eq. 18 and

$$S_{t'b}^{H^-} = (m_b - m_{t'})t_\beta V_{t'b} + f_\beta V_{t'b}\left[\left(m_{t'}\Sigma_{44}^{u*} - m_b\Sigma_{33}^d\right) + \left(m_t\Sigma_{34}^{u*}\frac{V_{tb}}{V_{t'b}} - m_{b'}\Sigma_{43}^d\frac{V_{t'b'}}{V_{t'b}}\right)\right],$$

$$P_{t'b}^{H^-} = (m_b + m_{t'})t_\beta V_{t'b} - f_\beta V_{t'b}\left[\left(m_{t'}\Sigma_{44}^{u*} + m_b\Sigma_{33}^d\right) + \left(m_t\Sigma_{34}^{u*}\frac{V_{tb}}{V_{t'b}} + m_{b'}\Sigma_{43}^d\frac{V_{t'b'}}{V_{t'b}}\right)\right],$$

$$S_{t's}^{H^-} = -P_{t's}^{H^-} = -m_{t'}t_\beta V_{t's} + f_\beta\left(m_{t'}V_{t's}\Sigma_{44}^{u*} + m_t V_{ts}\Sigma_{34}^{u*}\right) . \tag{51}$$

For the couplings $S_{t'b}^{H^-}$, $S_{t's}^{H^-}$, $P_{t'b}^{H^-}$, $P_{t's}^{H^-}$ we use the 4G2HDM Yukawa terms in the quark sector as given in [11], where Σ^u and Σ^d are the corresponding new mixing matrices in the up and down-quark sectors, respectively, obtained after diagonalizing the quarks mass matrices. In particular, adopting the type I 4G2HDM of [11], these matrices are given by

$$\Sigma_{ij}^d = D_{R,4i}^\star D_{R,4j} , \; \Sigma_{ij}^u = U_{R,4i}^\star U_{R,4j} , \tag{52}$$

in analogy with Eq. 16, where D_R, U_R are the rotation (unitary) matrices of the right-handed down and up-quarks, respectively. They can be approximated by (see [11])

$$\Sigma^d \simeq \begin{pmatrix} 0 & 0 & 0 & 0 \\ 0 & 0 & 0 & 0 \\ 0 & 0 & |\epsilon_b|^2 & \epsilon_b^\star \\ 0 & 0 & \epsilon_b & \left(1 - \frac{|\epsilon_b|^2}{2}\right) \end{pmatrix} , \; \Sigma^u \simeq \begin{pmatrix} 0 & 0 & 0 & 0 \\ 0 & 0 & 0 & 0 \\ 0 & 0 & |\epsilon_t|^2 & \epsilon_t^\star \\ 0 & 0 & \epsilon_t & \left(1 - \frac{|\epsilon_t|^2}{2}\right) \end{pmatrix} , \tag{53}$$

so that $\Sigma^{u,d} = 0$ if i or $j \neq 3, 4$, and the 34 blocks are parameterized by the quantities ϵ_b and ϵ_t. As in [11], a natural choice that we will adopt below is $\epsilon_b \sim m_b/m_{b'} << \epsilon_t$. Thus, neglecting terms of $\mathcal{O}(m_b/m_t)$ (and, therefore, neglecting also terms proportional to ϵ_b), the couplings $S_{t'b}^{H^-}$, $S_{t's}^{H^-}$, $P_{t'b}^{H^-}$, $P_{t's}^{H^-}$ can be approximated by

$$S_{t'b}^{H^-} = -P_{t'b}^{H^-} \approx \frac{m_{t'}}{t_\beta}V_{t'b} + m_t f_\beta \epsilon_t V_{tb} ,$$

$$S_{t's}^{H^-} = -P_{t's}^{H^-} \approx \frac{m_{t'}}{t_\beta}V_{t's} + m_t f_\beta \epsilon_t V_{ts} , \tag{54}$$

leading to $F_S^H \to 0$, $F_P^H \to 0$ and

$$F_A^H \approx \frac{i\,2f_{B_s}}{g^2}\left[\frac{S_{t's}^{H^-} S_{t'b}^{H^-*}}{M_{H^-}^2}\text{Re}\left(S_{\mu\nu'}^{H^-} P_{\mu\nu'}^{H^-*}\right)B_{HH}^A(y_{t'}, y_{\nu'})\right.$$

$$\left. + \frac{g}{\sqrt{2}m_W}\frac{m_{\nu'}m_{t'}}{m_W^2}\left\{V_{t'b}U_{24}^* S_{t's}^{H^-*}\left(S_{\mu\nu'}^{H^-} - P_{\mu\nu'}^{H^-}\right) + V_{t's}^* U_{24} S_{t'b}^{H^-}\left(S_{\mu\nu'}^{H^-*} - P_{\mu\nu'}^{H^-*}\right)\right\}B_{WH}^A(x_{t'}, x_{\nu'}, x_H)\right] \tag{55}$$

Notice that the term $U_{24}^* \cdot \left(S_{\mu\nu'}^{H^-} - P_{\mu\nu'}^{H^-}\right)$ is proportional to $(\delta_{U_2})^2$ and $\text{Re}\left(S_{\mu\nu'}^{H^-} P_{\mu\nu'}^{H^-*}\right)$ is proportional to both $(\delta_{U_2})^2$ and $(\delta_{\Sigma_2})^2$. Thus, there is a net effect in $B_s \to \mu\mu$ from the charged-Higgs box diagrams even when one of the small quantities that control the muon g-2 vanishes, i.e., when either $\delta_{U_2} \to 0$ or $\delta_{\Sigma_2} \to 0$, for which cases $[a_\mu]_{H^\pm}^{4G2HDM} \to 0$ (see Eq. 20). For example, for $\delta_{U_2} \to 0$ we have $[a_\mu]_{H^\pm}^{4G2HDM} \to 0$, while

$$F_A^H(\delta_{U_2} \to 0) \approx \frac{i\,f_{B_s}}{4}\frac{S_{t's}^{H^-} S_{t'b}^{H^-*}}{M_{H^-}^2}B_{HH}^A(y_{t'}, y_{\nu'})\frac{m_{\tau'}^2}{m_W^2}f_\beta^2|U_{44}|^2|\Sigma_{44}^\nu|^2|\delta_{\Sigma_2}|^2 , \tag{56}$$

The contributions from the charged Higgs exchange diagrams with (t, ν') can be obtained directly from Eqs. 47,48 and 49 by replacing t' with t, which eventually requires the replacements: $t' \leftrightarrow t$ and $\Sigma_{4\leftrightarrow3}^u$ in Eq. 51.

In Fig. 7 we plot the contribution to $BR(B_s \to \mu\mu)$ in the 4G2HDM from the box diagrams with the H^+ and (t, ν'), (t', ν') exchanges, as a function of ϵ_t (fixing $\epsilon_b = 0.01$) and $\lambda_{bs}^{t'} \equiv V_{t'b}V_{t's}^*$, for $m_{\nu'} = 100$, 200, 400 GeV, $m_{\tau'} = m_{\nu'}$ and $m_{H^+} = 500$ GeV. The allowed ranges of the key parameters δ_{U_2} and δ_{Σ_2}, which control the muon $g - 2$ in our model, are randomly chosen in the range $[0, 0.2]$ to be consistent with a_μ^{exp} given in Eq. 4. We also show the current experimental bound [31] and the SM predicted value for $BR(B_s \to \mu\mu)$. We see that the contribution from the new (i.e., in the 4G2HDM) box diagrams that involve the heavy 4th generation neutrino is consistent with the current experimental bound on $BR(B_s \to \mu\mu)$ for values of δ_{U_2} and δ_{Σ_2} that reproduce the observed muon $g - 2$. It is also interesting to note that both in the SM4 and in the 4G2HDM, $\text{Br}(B_s \to \mu^+\mu^-)$ can differ from the SM value by at-most a factor of O(3) in either direction.
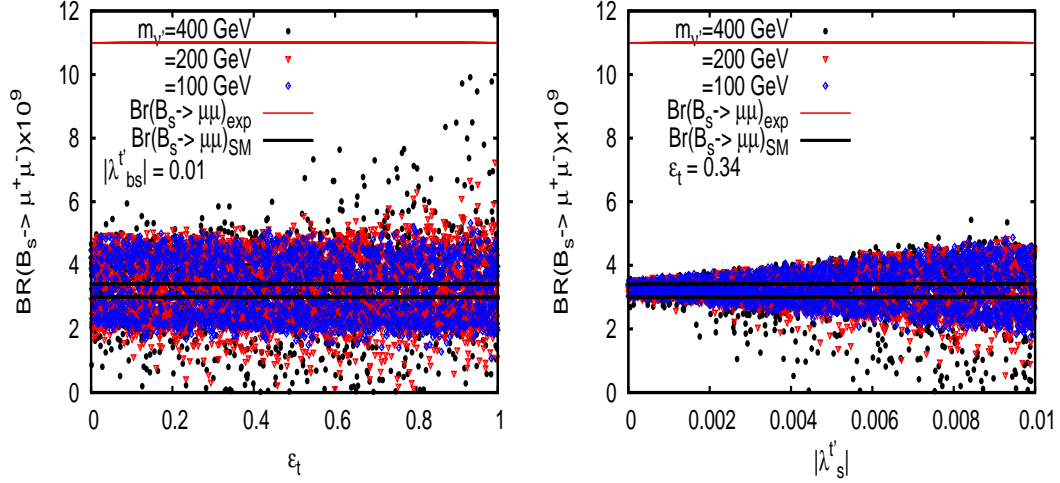
FIG. 7: $BR(B_s \to \mu\mu)$ in the 4G2HDM from box diagrams with the H^+ and (t, ν'), (t', ν') exchanges, as a function of ϵ_t (fixing $\epsilon_b = 0.01$) and $\lambda_{bs}^{t'} \equiv V_{t'b}V_{t's}^*$, for $m_{\nu'} = 100$, 200, 400 GeV, $m_{\tau'} = m_{\nu'}$ and $m_{H^+} = 500$ GeV. We considered only values of δ_{U_2} and δ_{Σ_2} which are allowed by a_μ given in Eq. 5, keeping both of them $\lesssim 0.2$. Also shown are the experimental 95% CL upper bound (upper/red horizontal line) and the SM predicted range (1σ) of values (lower/black horizontal lines).

V.   SUMMARY AND DISCUSSION

We have considered the effects of 1-loop exchanges of heavy 4th generation leptons on the muon $g - 2$, on the lepton flavor violating decays $\mu \to e\gamma$, $\tau \to \mu\gamma$ and on $B_s \to \mu^+\mu^-$, in the 4G2HDM which is a 2HDM where the Higgs doublet with the heavier VEV is coupled only to the 4th generation doublet while the "lighter" Higgs doublet is coupled to fermions of the 1st-3rd generations. This model is particularly motivated for the leptonic sector, as it effectively addresses the heaviness of a 4th generation EW-scale neutrino.

The muon $g - 2$ is sensitive in our model to the product $\delta_{U_2} \cdot \delta_{\Sigma_2}$, where $\delta_{U_2} \equiv \frac{U_{24}^*}{U_{44}^*}$, $\delta_{\Sigma_2} \equiv \frac{\Sigma_{42}^{e*}}{\Sigma_{44}^\nu}$, U_{ij} is the leptonic CKM-like PMNS matrix and Σ_{ij}^e, Σ_{ij}^ν are new mixing matrices in the charged and neutral leptonic sectors that are unique to the 4G2HDM.

We find that, depending on the mass $m_{\nu'}$, the experimentally measured muon magnetic moment can be accounted for if $\mathcal{O}(10^{-3}) \lesssim \delta_{U_2} \cdot \delta_{\Sigma_2} \lesssim \mathcal{O}(10^{-2})$. We also find that the decays $\mu \to e\gamma$ and $\tau \to \mu\gamma$ can have branching ratios which are not too far below the current bounds, i.e., of $\mathcal{O}(\text{few} \cdot 10^{-13})$ and $\mathcal{O}(\text{few} \cdot 10^{-9})$, respectively, if the products $\delta_{U_1} \cdot \delta_{\Sigma_2}$, $\delta_{U_2} \cdot \delta_{\Sigma_1} \sim \mathcal{O}(10^{-6})$ and $\delta_{U_2} \cdot \delta_{\Sigma_3}$, $\delta_{U_3} \cdot \delta_{\Sigma_2} \sim \mathcal{O}(10^{-3})$, respectively.

We also considered the effects of one-loop exchanges of the 4th generation heavy neutrino ν' on the decay $B_s \to \mu^+\mu^-$ and found that, in the four generations model considered here, $\text{BR}(B_s \to \mu^+\mu^-)$ can be larger or smaller than the SM predicted value by a factor of about three, for values of $\mathcal{O}(10^{-3}) \lesssim \delta_{U_2} \cdot \delta_{\Sigma_2} \lesssim \mathcal{O}(10^{-2})$, which render the observed value of the muon $g - 2$ to be consistent with the current upper limit on this decay.

[1] T. Kinoshita, M. Nio, Phys. Rev. **D70**, 113001 (2004); T. Kinoshita, M. Nio, Phys. Rev. **D73**, 013003 (2006); T. Kinoshita, M. Nio, Phys. Rev. **D73**, 053007 (2006); G. Gabrielse, D. Hanneke, T. Kinoshita, M. Nio, B. C. Odom, Phys. Rev. Lett. **97**, 030802 (2006); T. Aoyama, M. Hayakawa, T. Kinoshita, M. Nio, Phys. Rev. Lett. **99**, 110406 (2007); D. Hanneke, S. Fogwell, G. Gabrielse, Phys. Rev. Lett. **100**, 120801 (2008);

[2] G. Degrassi, G. F. Giudice, Phys. Rev. **D58**, 053007 (1998); A. Czarnecki, W. J. Marciano, A. Vainshtein, Phys. Rev. **D67**, 073006 (2003); S. Heinemeyer, D. Stockinger, G. Weiglein, Nucl. Phys. **B699**, 103-123 (2004); T. Gribouk, A. Czarnecki, Phys. Rev. **D72**, 053016 (2005);

[3] J. Prades, E. de Rafael, A. Vainshtein, In: Roberts, Lee B., Marciano, William J. (eds.):"Lepton dipole moments" 303-317, arXiv:0901.0306 [hep-ph]; M. Davier, A. Hoecker, G. Lopez Castro, B. Malaescu, X. H. Mo, G. Toledo Sanchez, P. Wang, C. Z. Yuan et al., Eur. Phys. J. **C66**, 127-136 (2010).

[4] C. Bouchiat and L. Michel, Phys. Rev. **106**, 170 (1957); M. Gourdin and E. De Rafael, Nucl. Phys. B **10**, 667 (1969).

[5] M. Davier, A. Hoecker, B. Malaescu, C. Z. Yuan and Z. Zhang, Eur. Phys. J. C **66**, 1 (2010).

[6] K. Hagiwara, A. D. Martin, D. Nomura and T. Teubner, Phys. Lett. B **649**, 173 (2007).

[7] F. Jegerlehner and A. Nyffeler, Phys. Rept. **477**, 1 (2009). A. Nyffeler, Phys. Rev. D **79**, 073012 (2009).

[8] See pdg minireview on muon g-2 in http://pdglive.lbl.gov.

[9] F. Jegerlehner and A. Nyffeler, Phys. Rept. **477** (2009) 1; For a recent update, see J. Prades, Acta Phys. Polon. Supp. **3**, 75 (2010).

[10] J. L. Lopez, D. V. Nanopoulos, X. Wang, Phys. Rev. **D49**, 366-372 (1994); U. Chattopadhyay, P. Nath, Phys. Rev. **D53**, 1648-1657 (1996); S. P. Martin, J. D. Wells, Phys. Rev. **D64**, 035003 (2001).

[11] S. Bar-Shalom, S. Nandi and A. Soni, Phys. Rev. D **84**, 053009 (2011)

[12] M.A. Luty, Phys. Rev. **D41**, 2893 (1990).

[13] G. D. Kribs, T. Plehn, M. Spannowsky and T. M. P. Tait, Phys. Rev. D **76**, 075016 (2007); M. S. Chanowitz, Phys. Rev. D **79**, 113008 (2009).

[14] G. W. S. Hou, arXiv:0810.3396 [hep-ph].

[15] M. Hashimoto and V. A. Miransky, Phys. Rev. **D81**, 055014 (2010).

[16] P. Q. Hung and C. Xiong, Phys. Lett. **B694**, 430 (2011).

[17] See e.g., A. Koryton (CMS collaboration), talk given at the EPS-HEP 2011, July 21-27, Grenoble, France.

[18] X.-G. He and G. Valencia, arXiv:1108.0222 [hep-ph].

[19] A. Soni, A. K. Alok, A. Giri, R. Mohanta and S. Nandi, Phys. Lett. B **683**, 302 (2010).

[20] A. Soni, A. K. Alok, A. Giri, R. Mohanta and S. Nandi, Phys. Rev. D **82**, 033009 (2010).

[21] A. J. Buras, B. Duling, T. Feldmann, T. Heidsieck, C. Promberger and S. Recksiegel, JHEP **1009**, 106 (2010).

[22] W. S. Hou and C. Y. Ma, Phys. Rev. **D82**, 036002 (2010).

[23] S. Nandi and A. Soni, Phys. Rev. D **83**, 114510 (2011)

[24] See also, M. Bobrowski, A. Lenz, J. Riedl and J. Rohrwild, Phys. Rev. D **79**, 113006 (2009); O. Eberhardt, A. Lenz and J. Rohrwild, Phys. Rev. D **82**, 095006 (2010).

[25] W. -S. Hou, F. -F. Lee, C. -Y. Ma, Phys. Rev. **D79**, 073002 (2009).

[26] J. P. Leveille, Nucl. Phys. **B137**, 63 (1978).

[27] See e.g., G. Burdman, L. Da Rold, R. D'Elia Matheus, Phys. Rev. **D82**, 055015 (2010).

[28] J. Adam *et al.* [MEG Collaboration], Phys. Rev. Lett. **107**, 171801 (2011).

[29] M. Blanke, A. J. Buras, B. Duling, A. Poschenrieder, C. Tarantino, JHEP **0705**, 013 (2007).

[30] M. Bona *et al.* (SuperB Collaboration), arXiv:0709.0451 [hep-ex].

[31] R. Aaij *et al.* (LHCb Collaboration), Phys. Lett. **B699**, 330 (2011); S. Chatrchyan *et al.* (CMS Collaboration), arXiv:1107.5834 [hep-ex], See also the public note LHCb-ANA-2011-039.

[32] T. Aaltonen *et al.* (CDF Collaboration), Phys. Rev. Lett. **107**, 239903 (2011) and Phys. Rev. Lett. **107**, 191801 (2011).

[33] H. E. Logan and U. Nierste, Nucl. Phys. B **586**, 39 (2000).

[34] G. Buchalla, A. J. Buras, Nucl. Phys. **B400**, 225-239 (1993).

[35] M. Misiak, J. Urban, Phys. Lett. **B451**, 161-169 (1999).